

CASE FILE COPY

NATIONAL ADVISORY COMMITTEE FOR AERONAUTICS

WARTIME REPORT

ORIGINALLY ISSUED

February 1945 as
Advance Restricted Report 5A03a

AN INVESTIGATION OF A THERMAL ICE-PREVENTION SYSTEM

FOR A C-46 CARGO AIRPLANE

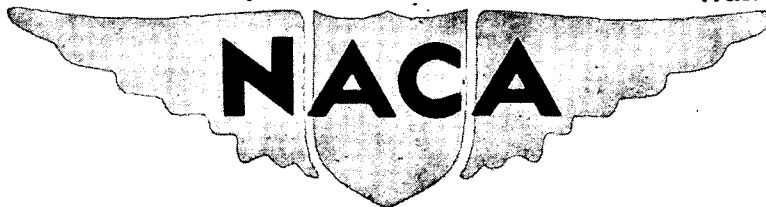
II - THE DESIGN, CONSTRUCTION, AND PRELIMINARY
TESTS OF THE EXHAUST-AIR HEAT EXCHANGER

By Richard Jackson

387
Ames Aeronautical Laboratory
Moffett Field, California

FILE COPY

To be returned to
the files of the National
Advisory Committee
for Aeronautics
Washington, D. C.



WASHINGTON

NACA WARTIME REPORTS are reprints of papers originally issued to provide rapid distribution of advance research results to an authorized group requiring them for the war effort. They were previously held under a security status but are now unclassified. Some of these reports were not technically edited. All have been reproduced without change in order to expedite general distribution.

NATIONAL ADVISORY COMMITTEE FOR AERONAUTICS

ADVANCE RESTRICTED REPORT

AN INVESTIGATION OF A THERMAL ICE-PREVENTION SYSTEM
FOR A C-46 CARGO AIRPLANE

II -- THE DESIGN, CONSTRUCTION, AND PRELIMINARY
TESTS OF THE EXHAUST-AIR HEAT EXCHANGER

By Richard Jackson

SUMMARY

As a part of a comprehensive investigation of a thermal ice-prevention system for a C-46 cargo airplane, an exhaust-air heat exchanger has been designed, constructed, and flight-tested at the Ames Aeronautical Laboratory. The research was undertaken to provide the C-46 airplane with a satisfactory source of heated air and to continue the development of the heat exchanger as a part of thermal ice-prevention equipment.

The results of the heat-exchanger tests indicate that the required thermal output and desired air-temperature rise have been achieved and that the exchanger is suitable for use in the C-46 airplane.

INTRODUCTION

This report is the second in a series which describe a comprehensive investigation of a thermal ice-prevention system for a C-46 airplane. The establishment of data on the design of the exhaust-air heat exchanger has been undertaken as an important part of the investigation of the thermal ice-prevention system. In the investigation of the equipment for the C-46 airplane, additional information was sought on design and construction methods and the reliability with which the exchanger performance can be predicted from calculations.

The components and arrangement of the C-46 airplane equipment of which the exchangers are a part are shown in figure 1. The required performance of the exchangers was established in the analysis of the system which is described in reference 1. Flight tests of several exchangers at the Ames Aeronautical Laboratory (reference 2) and an extensive laboratory investigation by the University of California (references 3 to 10) have indicated that a plate-type cross-flow exchanger may be employed as a practical source of heated air for thermal ice-prevention equipment, and have established important theoretical relationships for predicting the exchanger performance. Although considerable design information on diffusers and bends in ducts was found in the literature, very little information regarding the design of converging and diverging bends, which are necessarily associated with the inlet and outlet headers for cross-flow heat exchangers, was available. Therefore, it was necessary to employ a design procedure which would result in efficient headers for use with the heat exchanger.

The purpose of this research was to design, construct, and test a plate-type cross-flow heat exchanger, complete with inlet and outlet headers, which would satisfactorily meet the requirements of the thermal ice-prevention system of the C-46 airplane, as described in reference 1.

This investigation has been undertaken at the request of and with the cooperation of the Air Technical Service Command, Army Air Forces. Acknowledgment is given to the valuable assistance rendered the Ames Laboratory by the Solar Aircraft Corporation in the fabrication of the exchanger and exhaust-duct parts.

SYMBOLS

- A cross-sectional free area, square feet
- c_p specific heat of fluid, British thermal unit per pound,
 degree Fahrenheit
- d fluid passage gap, feet
- D_e equivalent diameter of fluid passage, feet
- f friction factor for fluid flow

| | |
|------------|---|
| g | gravitational acceleration (32.2), feet per second, second |
| G | weight rate of fluid flow per unit cross-sectional area (W/A), pounds per hour, square foot |
| h | surface heat-transfer coefficient, British thermal units per hour, square foot, degree Fahrenheit |
| k | thermal conductivity of fluid, British thermal unit per hour, square foot, degree Fahrenheit per foot |
| K | constant, or factor |
| L^i | over-all passage length, feet |
| L | effective passage length, feet |
| L_N | no-flow dimension, feet |
| n | number of fluid passages |
| Nu | Nusselt number (hD_e/k) |
| p | pressure, pounds per square foot |
| Δp | pressure difference, pounds per square foot |
| q | dynamic pressure, or velocity head, pounds per square foot |
| Q | rate of heat flow, heat output, or enthalpy change, British thermal units per hour |
| R | gas constant (53.3), feet per degree Fahrenheit |
| Re | Reynolds number (GD_e/μ) |
| S | heat-transfer surface area, square feet |
| t | temperature, degrees Fahrenheit |
| Δt | temperature difference, degrees Fahrenheit |
| T | absolute temperature ($t + 460$), degrees Fahrenheit absolute |

U over-all heat-transfer coefficient, British thermal units per hour, square foot, degree Fahrenheit

W weight rate of fluid flow, pounds per hour

Y specific weight of fluid, pounds per cubic foot

ρ mass density of fluid (γ/g), slugs per cubic foot

μ absolute viscosity of fluid, pounds per hour, foot

Subscripts

a air side

av average conditions

c core

CF cross flow

E expansion

F surface friction

g gas side

in inlet conditions

L logarithmic mean

m momentum

o free-stream conditions

out outlet conditions

T total pressure

S static pressure

1, 2, 3, 4, 5, and 6 refer to stations shown in figure 13

ANALYTIC DESIGN OF HEAT-EXCHANGER CORE

The general arrangement of the thermal ice-prevention system proposed for the C-46 airplane is shown in figure 1.

The configuration of the engine-exhaust system prescribed the use of four heat exchangers, and the experimental nature of the investigation demanded an installation which involved a minimum of alterations to the airplane. Therefore it was decided to install the heat exchangers on the airplane as shown in figure 2. This location of the heat exchangers arbitrarily fixed the allowable core dimensions approximately as follows: gas-passage length - 15 inches, air-passage length - 10 inches, no-flow dimension - 9 inches. The location also restricted the choice of inlet and outlet headers for this installation.

A flat-plate-type core was chosen primarily for aerodynamic reasons. Previous experience had shown that low air-side pressure losses were of utmost importance, and since the ratio of useful to nonuseful losses in a flat-plate-type core is a maximum, this type was chosen as that which would have the lowest core-pressure losses for a given rate of heat transfer. Other factors considered in choosing a core type for the C-46 airplane exchanger were as follows: the flat-plate type is readily designed and fabricated; the ratios of heat output to core size and weight for this type compare favorably with those of other types (reference 2) and although very little service life data were available, the existing data indicated that the service characteristics of a well-designed, flat-plate exchanger would probably be satisfactory.

The thermal ice-prevention equipment for the C-46 airplane was designed for conditions which exist in long-range cruising flight at a pressure altitude of 18,000 feet. This criterion has been used with success in the design of similar equipment for other airplanes. Preliminary tests were made with the unmodified airplane at Ames Laboratory (reference 1) to establish pressure-distribution data at this flight condition, necessary for the design of the wing and empennage equipment. During these tests it was found that the engines were operated at 2000 rpm and 29 inches manifold pressure and that the indicated airspeed was about 155 miles per hour. The exhaust-gas temperature, measured just ahead of the proposed heat-exchanger location, was approximately 1600° F. Calculations based on the engine displacement (2800 cu in.) indicated that the weight rate of exhaust gas per heat exchanger would be approximately 3200 pounds per hour. The results of an analysis of the thermal requirements of the wings, empennage, and windshield (reference 1) based on the pressure-distribution data obtained in the above-mentioned tests showed that each heat exchanger should be capable of

raising the temperature of 4130 pounds of air per hour from 0° to 300° F resulting in a heat output of 300,000 Btu per hour at design conditions.

The most important single factor affecting the heat-exchanger design was the restriction that the over-all air-side pressure loss of the entire system must not exceed the free-stream dynamic pressure. Compliance with this restriction eliminated the need for auxiliary air pumps in various parts of the system. It was obvious that a small amount of additional ram would be obtained by locating the air scoop in the propeller slipstream and it was probable that a small negative pressure would occur in the region in which the air left the wing. These unknown factors were not considered in this design but were looked upon as providing a margin of safety. The free-stream dynamic pressure at the design speed of 155 miles per hour is about 60 pounds per square foot. Of this available ram, one-half (30 lb/sq ft) was arbitrarily considered the allowable air-side pressure loss of the heat-exchanger installation, which includes the inlet header, exchanger core, and outlet header. It was further arbitrarily assumed that the allowable pressure loss of each of these three components of the exchanger installation was one-third of the total, or 10 pounds per square foot.

The increment of engine-back pressure added by an exhaust-air heat exchanger is relatively unimportant unless this value becomes so great as to cause a material reduction in engine power. The allowable value of this increment is dependent upon the particular engine-exhaust system involved, and as yet no suitable method for determining the allowable gas-side pressure drop of a heat-exchanger installation has been established. In the absence of a definite allowable value, therefore, it was decided to make the gas-side pressure drop of the exchanger core as low as was reasonably possible.

The design conditions which have been established above are summarized in the following table:

| | | |
|---------------------------------------|----------------------|-----------------|
| Pressure altitude | 18,000 feet | |
| Indicated airspeed | 155 miles per hour | |
| Heat output | 300,000 Btu per hour | |
| | <u>Air side</u> | <u>Gas side</u> |
| Flow rate, lb per hr | 4130 | 3200 |
| Inlet temperature, °F | 0 | 1600 |
| Outlet temperature, °F | 300 | ----- |
| Allowable pressure drop: | | |
| Over-all, lb per sq ft | 30 | ----- |
| Inlet header, lb per sq ft | 10 | ----- |
| Core, lb per sq ft | 10 | ----- |
| Outlet header, lb per sq ft | 10 | ----- |

Typical air and gas passages assumed for the analytical design of the heat-exchanger core are shown in figure 3. The procedure followed in the design was a trail-and-error process in which values of L'_a , L'_g , d_a , and d_g (fig. 3) were assumed, substituted in the following heat-transfer relationships, and adjusted as necessary to obtain a heat balance. The heat-transfer relationships used were taken from reference 11 and are listed below:

$$Q = W_a c_{p_a} \Delta t_a \dots \dots \dots \text{Air-side enthalpy change} \quad (1)$$

$$Q = W_g c_{p_g} \Delta t_g \dots \dots \dots \text{Gas-side enthalpy change} \quad (2)$$

$$Q = U S \Delta t_L \dots \dots \dots \text{Over-all heat-transfer rate} \quad (3)$$

$$U = \frac{1}{1/h_a + 1/h_g} \dots \dots \dots \text{Over-all heat-transfer coefficient} \quad (4)$$

(The thermal resistance of the metal walls is negligible.)

$$Nu = hD_e/k = 0.02 Re^{0.8} \dots \dots \dots \text{Nusselt number} \quad (5)$$

$$h = Nu k/D_e \dots \dots \dots \text{Surface heat-transfer coefficient} \quad (6)$$

$$\Delta t_L = K_{CF} \frac{(t_{g_{in}} - t_{a_{in}}) - (t_{g_{out}} - t_{a_{out}})}{\log_e(t_{g_{in}} - t_{a_{in}}) / (t_{g_{out}} - t_{a_{out}})} \dots \dots \dots \text{Logarithmic mean-temperature difference} \quad (7)$$

(The cross-flow correction factor K_{CF} was assumed equal to unity.)

Relationship 5 is strictly applicable only to the turbulent flow of gases through round tubes, but has been proved satisfactory for tubulent flow through rectangular channels when an equivalent diameter $D_e = \frac{4 \times \text{free area}}{\text{wetted perimeter}}$ is used. When a heat balance had been established, the assumed dimensions then were used to determine the pressure drops in the system by means of the following relationships:

$$\Delta p_F = f_{av} q_{av} \frac{4L}{D_e} \dots \dots \dots \text{friction total-pressure drop} \quad (1)$$

$$\Delta p_E = K_E q_4 \dots \dots \dots \text{expansion total-pressure drop} \quad (2)$$

$$K_E = (1 - A_c/A_s)^2 \dots \dots \dots \text{expansion factor} \quad (3)$$

$$\Delta p_m = q_4 - q_3 \dots \dots \dots \text{momentum total-pressure drop} \quad (4)$$

(The entrance contraction loss was assumed to be negligible.)

These relationships were also based on information found in reference 11, but have been revised to suit the nomenclature of this report. The air-side momentum pressure drop (Δp_m) is the result of a transformation of energy and is not necessarily a loss of total head. It may be regained in the form of total pressure, provided the air is cooled to its original temperature at the same Reynolds number. Although it is probable that Δp_m is partially recovered in the system aft of the heat exchanger, it is slightly conservative to consider it as a real loss of total head. On the gas side the momentum change results in a gain in total head, but generally the magnitude of Δp_m is insignificant when compared with the over-all pressure change. The procedure described above, and used in the analytical design of the heat-exchanger core, is illustrated in the sample calculations given in table I.

The design calculations resulted in the choice of a heat-exchanger core consisting of 19 air passages with 3/16-inch gaps and 18 gas passages with 1/4-inch gaps. The over-all gas-passage length, air-passage length, and no-flow dimension of this heat exchanger were 15 by 9½ by 8½ inches, respectively. The calculated performance of this heat-exchanger core at design conditions was as follows:

Heat output - 325,000 Btu per hour

Air-temperature rise - 328° F

Air-side total-pressure drop - 12 pounds per square foot

Gas-side total-pressure drop - 22 pounds per square foot

A wood mock-up of this heat exchanger (fig. 4) was constructed for the purpose of verifying the air-side pressure-drop calculations and also for use in tests of several air-inlet and -outlet headers. The peculiar plan form of the heat-exchanger plates was the result of an arbitrary choice and has little justification except that this plan form was slightly more adaptable to the C-46 airplane installation than an equivalent rectangular shape. Values of isothermal air-side pressure drop measured in tests with the wood mock-up were in close agreement with the predictions for the heat exchanger, and it was concluded that the pressure-drop calculations were satisfactory. The next step in the design procedure was the construction of an exchanger core from cold-rolled-steel sheets (fig. 5). Cold-rolled steel was used because stainless steel was not available in sufficient quantities at the time, and also because this exchanger was to be used only for test purposes and consideration of the service life was relatively unimportant. This exchanger was tested isothermally in the laboratory and nonisothermally in flight on an C-47A airplane. The results of these tests, which have been reported in reference 2, indicated that the design procedure used herein was satisfactory, and at the same time disclosed certain structural weaknesses in the exchanger core. These weaknesses are described in the section under Preliminary Tests. An analysis of the test data revealed that the air-side and gas-side pressure drop could be reduced slightly by omitting two air and gas passages and expanding the remaining passage gaps to fill out the original over-all dimensions. The effect of this modification on heat output was a reduction from 325,000 to 300,000 Btu per hour. The revisions suggested by the test results for this heat exchanger, model 1, were incorporated in a revised design, model 2, which is shown in figures 6 and 7. Four heat exchangers were constructed as shown in figure 6 for the C-46 airplane.

SELECTION OF INLET AND OUTLET HEADERS

There was no simple design procedure to be followed in the selection of the inlet and outlet headers for the heat

exchanger installation on the C-46 airplane. Considerable data on constant area turns, straight diffusers, and on diffuser-resistance combinations were found in available literature, but there was a scarcity of data on diverging and converging turns which are necessarily a part of the inlet and outlet headers for a cross-flow heat exchanger. Furthermore, the size and shape of the headers were limited by the location of the exchanger core on the airplane. It was decided, therefore, to use the existing data on turns and diffusers as a guide in determining the approximate shape of the headers that could be used in this installation and then to resort to laboratory tests for the final selection.

A skeleton mock-up of the engine nacelle, back to the front spar of the wing, was constructed and the mock-up of the heat-exchanger core was installed in its proper location. It was found that the core could be mounted in such a manner that the air-side headers need to turn the air only through approximately 45° instead of the anticipated 90° . The approximate size and shape of the air-inlet header were determined from the mock-up, and several possible air-side inlet headers were constructed. These were tested isothermally in conjunction with the core mock-up and it was found that, owing to the particular location of the core, most of the turning occurred in a region of very low velocity (27 ft/sec at design conditions) and consequently the turning losses were small. Therefore, it was necessary only to choose a reasonable expansion angle and an inlet area which would afford a reasonable inlet velocity ratio. The use of turning vanes in the inlet header, although desirable from the viewpoint of insuring an adequate supply of cooling air to the hot upstream end of the heat-exchanger core, was eliminated because of the undesirable complications involved in keeping the leading edges of the vanes free from ice. Thus, since the actual shape of the inlet header was not very critical, the shape finally chosen (fig. 8) was determined principally by considerations such as the necessity for cooling the ball joint and for locating the header entrance at a sufficient distance away from the nacelle to prevent the low-velocity boundary-layer air adjacent to the nacelle surface from entering the inlet header.

The selection of an air-side outlet header was more involved. From the nacelle mock-up it was at first decided to lead the air from the heat exchanger into a duct extending through a fire wall. A plaster of paris mold for the outlet header was formed in the mock-up with as reasonable a

shape and bend radius as possible. A sheet-metal header was patterned after this mold and is shown as outlet 2-A in figure 9. This header was tested with and without turning vanes (outlets 2-B and 2-A, respectively, fig. 9). The pressure loss of the header without vanes was less than that with vanes and was well below the allowable loss (3.5 lb/so ft at standard sea-level conditions) and therefore was considered satisfactory. The vanes used in outlet 2-B were not designed but were chosen arbitrarily and this is probably the reason they added to the head loss. However, since they were unnecessary, no attempt was made to improve them. Although outlet 2-A was satisfactory for the first proposed installation, considerations involving revisions to major structural members in the nacelle and of relocating equipment housed in the nacelle made it desirable to duct the air along the outside of the nacelle to the wing leading edge. The outlet header was, therefore, revised to meet this new requirement and is shown as outlet 3 in figure 9. Although outlet 3 had a higher air-flow resistance than outlets 2-A and 2-B, the resultant pressure drop was only slightly above the allowable value and further improvements were curtailed by a lack of time.

The location of the exchangers (fig. 2) allowed little choice in selecting the gas-side headers. The gas-side inlet header was merely a transition from the 8-inch-diameter ball joint to the $8\frac{1}{2}$ - by $9\frac{1}{2}$ -inch cross section of the exchanger core. The shape of the exhaust outlet (figs. 2 and 8) was determined as follows: A plaster mold of the outlet was formed in the mock-up of the nacelle and was shaped so as to duct the exhaust gas away from the exchanger core into the free-air stream in as short a path as possible. It was necessary to curve the mold outward to circumvent structural members in the nacelle, and the exit area (0.17 so ft) was chosen to coincide with the exit area of the original exhaust stack. The dies for forming the exhaust outlet were patterned after this plaster mold.

STRUCTURAL DESIGN AND FABRICATION OF HEAT EXCHANGER

Previous experience with plate-type heat exchangers indicated that the plate material should be either stabilized stainless steel or Inconel. A minimum metal thickness of 0.032 inch was selected to allow for thinning in the drawn parts of the plates. It was decided to draw beads, extending

into the air passages, into the plates to act as plate stiffeners and air-passage spacers. The beads were placed in the air passages parallel to the air flow to minimize the air-side pressure losses. The gas-passage gap was to be maintained by means of dimples drawn into the plates and extending into the gas passages. These beads and dimples are illustrated in figure 5. The leading and trailing edges of the air and gas passages were beveled and a 3/8-inch flange was left to provide a means of joining the adjacent plates. The corner construction is shown in detail (b) of figure 6. The overlapping tabs on adjacent plates shown in the detail were used to provide additional strength in the corners. Steel dies were used to form the plates, as described above. The leading edges exposed to the gas stream were provided with 0.043-inch abrasion caps (detail (a), fig. 6) to protect the plate edges from excessive wear and corrosion caused by solid particles in the high-velocity gas stream.

The plates were assembled into a heat-exchanger core in the following manner:

1. The beads of adjacent plates were welded together by means of overlapping spot welds, thereby forming one air passage.
2. The flanges in the gas stream then were spot-welded with overlapping spots and the overlapping tabs were welded together.
3. The gas-side leading-edge abrasion caps were spot-welded in place.
4. The individual air passages then were welded together along the air-side leading edges. Overlapping spot welds were used here also.
5. Flame welding was used at all points not spot-welded and also was used along all the leading and trailing edges to reinforce the spot welds.

The weight of the heat-exchanger core when completely assembled was 52.5 pounds.

The gas-side inlet and outlet headers were formed on a drop hammer. Each was formed in two halves from 0.040-inch stainless steel and the halves were flame-welded together. The complete headers then were flame-welded to the exchanger core. The air-side inlet and outlet headers were hand-worked.

The inlet header was made from 0.032-inch, 3S $\frac{1}{2}$ H aluminum sheet and the joints were fastened with countersunk aluminum rivets. The outlet header was made from 0.020-inch stainless steel and was flame-welded at the joints. The air-side headers were attached to the exchanger core by means of self-locking plate nuts as shown in figure 2. The inlet and outlet headers used in the heat-exchanger installation on the C-46 airplane are shown in figure 8.

PRELIMINARY TESTS

Heat exchanger, model 1, was tested isothermally in the laboratory and nonisothermally in flight on a North American O-47A airplane. A description of these tests has been reported in detail in reference 2, in which model 1 was designated heat exchanger 48. The plates of this exchanger buckled severely within 10 hours of flight, and thereby indicated that the plates should be reinforced in the gas-flow direction. Therefore in the revised design, model 2, longitudinal hat section stiffeners, made from 0.025-inch stainless steel were spot-welded to each plate of the heat exchanger as shown in figures 6 and 7. The dimples used in the previous models were omitted in model 2 as the stiffeners also served as the gas-passage spacers. Heat exchanger, model 2, was not tested isothermally but was tested in flight on an O-47A airplane. The installation used in the tests of this exchanger on the O-47A airplane is shown in figure 10. The procedure followed in the flight tests was the same as that used in the tests of model 1 and is described briefly as follows: During the tests at 5000 feet level flight was maintained and the engine power was held constant at a value which corresponded to a gas-flow rate of approximately 3300 pounds per hour. The fuel-air ratio was adjusted until the indicated gas temperature at the gas inlet header (station 6, fig. 10) was steady at 1600° F. The air-flow rate was then varied in steps to cover a range of flows above and below the design value of 4130 pounds per hour. Sufficient instrumentation, as indicated in figure 10, was provided to obtain, at each air-flow rate, measurements of inlet and outlet temperatures of the air and gas streams, gas-side static pressures at stations 6 and 7, air-side static pressures at stations 1 and 4, air-side total pressure at station 1, and air-side total-pressure drop between stations 2 and 3. In one flight at 5000 feet the engine power was increased and the gas-flow rate during this test was approximately 4400 pounds per hour. The same general procedure was followed during a flight at 18,000 feet, except that the gas-flow rate was limited to 2500 pounds per hour by the capacity of the engine at that altitude.

RESULTS AND DISCUSSION

Performance data for both heat exchangers, models 1 and 2, were evaluated from the test results and are presented in figure 11. The values of heat output shown in this figure consist of air-side enthalpy changes ($Q = W_a c_{p_a} \Delta t_a$). The changes of enthalpy on the gas side consistently ran about 15 percent higher than those on the air side. The air-side total-pressure drop of the model 2 exchanger core was measured directly during the flight tests. The over-all total-pressure drop for exchanger, model 2, includes the duct and header losses between stations 1 and 4 (fig. 10) on the air side and between stations 6 and 7 on the gas side. The over-all values for exchanger, model 1, include similar pressure losses which are defined in reference 2. The values of over-all total-pressure drop were obtained in the following manner: The total pressures at stations 1, 4, 6, and 7 (fig. 10) were determined by adding the calculated dynamic pressure

$$\left(q = \left[\frac{W}{3600A} \right]^2 \times \frac{1}{2gY} \right) \text{ at each station to the measured}$$

static pressure at the corresponding stations. The total-pressure drop was then obtained as the difference between the total pressures at the stations involved. Although this method is exact only when there is no change in velocity distribution between the two stations, the error caused by such changes is negligibly small, provided the flow is turbulent throughout the path between the stations.

The excessive gas-side pressure drop shown in figure 11 for exchanger, model 2, at 18,000 feet was probably caused by the particular installation used on the O-47A airplane. Although it is not shown in figure 10, the exhaust outlet shown in figure 8 was attached to the core and was enclosed by the tail pipe. The calculated gas-side core and outlet-header pressure drop amounts to approximately 60 pounds per square foot at a flow rate of 3200 pounds per hour and at an altitude of 18,000 feet. The value indicated by the test data is about 110 pounds per square foot. The difference (50 lb/sq ft) can be reasonably attributed to expansion losses in the inlet header and to probable adverse effects in the region where the gas leaves the outlet attached to the core and enters the $7\frac{1}{2}$ -inch-diameter tail pipe.

A comparison between the measured and the calculated heat output and air-side core total-pressure drop for heat exchanger, model 3, is given in figure 12. A similar comparison for the gas-side pressure drop was omitted because the gas-side core pressure drop was not measured. The measured heat output and core pressure drop at an altitude of 5000 feet are in close agreement with the calculated values. The scattering of the measured pressure-drop data at 18,000 feet is inexplicable, but even with the scattering the test points are sufficiently close to the calculated curve to indicate that the method of calculation is satisfactory.

The heat output data measured at 5000 feet with a gas-flow rate of 4400 pounds per hour were plotted in figure 12 for comparative purposes. The data indicate that when the gas-flow rate is reduced from 3300 to 2500 pounds per hour the reduction in heat output is small; yet when the gas-flow rate is increased to 4400 pounds per hour the heat output is noticeably increased. The geometry of the heat-exchanger core is such that the unit thermal conductance is increased perceptibly by increasing the gas-flow rate above the design value, but is reduced only slightly by an equivalent reduction below the design value. Therefore, it may be expected that during a let-down at reduced power, while flying in icing weather, the heat output from the exchangers will remain sufficiently high to afford adequate protection.

It is notable that the thermal performance of the heat exchanger is practically unaffected by changes in altitude when the fluid-flow rates are maintained. This phenomenon is readily explained by the fact that the important fluid properties involved in the heat-transfer relationships (c_p , μ , and k) are affected but slightly by pressure changes of the order encountered, and that the change in average temperature with altitude is too small to affect materially the values of these fluid properties or the value of the logarithmic mean-temperature difference. On the other hand the effect of changes in altitude on pressure drop at constant fluid-flow rates is very marked. The pressure drop of any component part of an installation varies inversely with the density ratio applicable to that particular part. If, for example, a and b denote flights at different altitudes but with the same fluid-flow rates and if $(\Delta p_c)_a = (\Delta p_F)_a + (\Delta p_E)_a + (q_{out} - q_{in})_a$ is the drop in total pressure of a heat-exchanger core at flight condition a , then at flight condition b

$$\begin{aligned}
 (\Delta p_c)_b &= (\Delta p_F)_a \frac{(\rho_{av})_a}{(\rho_{av})_b} + (\Delta p_E)_a \frac{(\rho_{out})_a}{(\rho_{out})_b} \\
 &+ \left[(q_{out})_a \frac{(\rho_{out})_a}{(\rho_{out})_b} - (q_{in})_a \frac{(\rho_{in})_a}{(\rho_{in})_b} \right]
 \end{aligned}$$

The change in Reynolds number, and therefore the friction factor (f), with temperature is assumed to be negligible in the foregoing relationships. This idea may be expressed in another way which is more directly applicable to estimations of the performance of thermal ice-prevention equipment at various altitudes. For a given system on an airplane flying at the same indicated airspeed at various altitudes, as a rough approximation, the air-flow rate through the installation will vary inversely as the square root of the density ratio. (The density applicable here is the average density of the air within the heat exchanger.) Thus, for a given system the air-flow rate decreases rapidly with increases in altitude. This results in a decrease in heat output, an increase in the air-side temperatures, and a general increase in the metal temperatures within the heat exchanger. All of these changes are undesirable in a thermal ice-prevention system. Particular care, therefore, must be taken in the design of each part of the system to provide an adequate supply of air for cooling the exchanger core and to prevent overheating of the structural members of the lifting surfaces; otherwise serious failures may occur at the higher altitudes, especially at high-power conditions.

The distribution of air-side pressure losses in the final heat-exchanger installation is shown in figure 13. The over-all pressure drop from station 1 to station 6 is 26 pounds per square foot, or 42 percent of the free-stream dynamic pressure (q_0). This is slightly lower than the allowable value of $0.5q_0$ and is therefore satisfactory. However, the core pressure drop (station 2 to station 5) is only 11.3 pounds per square foot and of this amount the useful friction pressure drop is only 4.8 pounds per square foot or 8 percent of q_0 . Thus the nonuseful losses in this installation amount to about 34 percent of the available ram and obviously should be reduced. The

outlet header accounts for about $0.16q_0$; while the inlet header and the expansion loss at the trailing edge of the core account for about $0.07q_0$ each. Through careful design each of these three losses can be reduced. Such a reduction may be utilized as a reduction in the required pumping horsepower, or may be added to the allowable friction pressure drop of the core, thereby making possible the choice of a smaller and lighter heat exchanger.

The curve of static-pressure variation was plotted on this figure merely as a matter of interest; the difference between the two curves at any point is the local velocity head at that point.

CONCLUSIONS

The analytic and test data contained herein clearly indicate the following conclusions:

1. The analytic design procedures used in this report have been proved satisfactory.
2. The selected exchanger core and headers successfully meet the requirements of the thermal ice-prevention system for the C-46 airplane.
3. The performance of the heat-exchanger installation can be greatly improved through the reduction of the non-useful pressure losses associated with the outlet header, the inlet header, and the expansion at the trailing edges of the exchanger core.

Ames Aeronautical Laboratory,
National Advisory Committee for Aeronautics,
Moffett Field, Calif.

REFERENCES

1. Neel, Carr B., Jr.: An Investigation of a Thermal Ice-Prevention System for a C-46 Cargo Airplane. I - Analysis of the Thermal Design for Wings, Empennage, and Windshield. NACA ARR No. 5AO3, 1945.
2. Jackson, Richard, and Hillendahl, Wesley H.: Flight Tests of Several Exhaust-Gas-To-Air Heat Exchangers. NACA ARR No. 4C14, 1944.
3. Tribus, Myron, and Boelter, L. M. K.: An Investigation of Aircraft Heaters. II - Properties of Gases. NACA ARR, Oct. 1942.
4. Martinelli, R. C., Morrin, E. H., and Boelter, L. M. K.: An Investigation of Aircraft Heaters. VII - Thermal Radiation from Athermanous Exhaust Gases. NACA ARR, Dec. 1942.
5. Boelter, L. M. K., Miller, M. A., Sharp, W. H., Morrin, E. H., Iversen, H. W., and Mason, W. E.: An Investigation of Aircraft Heaters. IX - Measured and Predicted Performance of Two Exhaust Gas-Air Heat Exchangers and an Apparatus for Evaluating Exhaust Gas-Air Heat Exchangers. NACA ARR, March 1943.
6. Boelter, L. M. K., Dennison, H. G., Guibert, A. G., and Morrin, E. H.: An Investigation of Aircraft Heaters. X - Measured and Predicted Performance of a Fluted-Type Exhaust Gas and Air Heat Exchanger. NACA ARR, March 1943.
7. Boelter, L. M. K., Miller, M. A., Sharp, W. H., and Morrin, E. H.: An Investigation of Aircraft Heaters. XI - Measured and Predicted Performance of a Slotted-Fin Exhaust Gas and Air Heat Exchanger. NACA ARR No. 3D16, 1943.
8. Boelter, L. M. K., Dennison, H. G., Guibert, A. G., and Morrin, E. H.: An Investigation of Aircraft Heaters. XII - Performance of a Formed-Plate Crossflow Exhaust Gas and Air Heat Exchanger. NACA ARR No. 3E10, 1943.

9. Boelter, L. M. K., Guibert, A. G., Miller, M. A., and Morrin, E. H.: An Investigation of Aircraft Heaters. XIII - Performance of Corrugated and Noncorrugated Fluted Type Exhaust Gas-Air Heat Exchangers. NACA ARR No. 3H26, 1943.
10. Boelter, L. M. K., Morrin, E. H., Martinelli, R. C., and Poppendiek, H. F.: An Investigation of Aircraft Heaters. XIV - An Air and Heat Flow Analysis of a Ram-Operated Heater and Duct System. NACA ARR No. 4C01, 1944.
11. McAdams, William H.: Heat Transmission. McGraw-Hill Book Co., Inc., 2d ed., 1942.

TABLE I.- SAMPLE CALCULATIONS
C-46 Airplane

| BASIC DESIGN DATA | AIR SIDE | GAS SIDE |
|---|----------|----------|
| Weight rate (W), lb/hr | 4130 | 3200 |
| ¹ Inlet temperature (t ₃), °F | 0 | 1600 |
| Outlet temperature (t ₄), °F | 300 | 1300 |
| Average temperature (t _{av}), °F | 150 | 1450 |
| Specific heat at t _{av} (c _p), Btu/(lb)(°F) | 0.241 | 0.30 |
| Absolute viscosity at t _{av} (μ), lb/(hr)(ft) | 0.049 | 0.10 |
| Thermal conductivity at t _{av} (k), Btu/(hr)(sq ft)(°F/ft) | 0.017 | 0.045 |
| Absolute pressure (p ₀), lb/sq ft | 1060 | 1060 |
| Specific weight at t ₃ (γ ₃), lb/cu ft | 0.0432 | 0.0097 |
| Specific weight at t _{av} (γ _{av}), lb/cu ft | 0.0326 | 0.0104 |
| Specific weight at t ₄ (γ ₄), lb/cu ft | 0.0262 | 0.0113 |
| ² Logarithmic mean-temperature difference (Δt _L), °F = $\frac{(1600 - 0) - (1300 - 300)}{\log_e 1600/1000}$ | | 1375 |
| HEAT TRANSFER | | |
| Over-all passage length (L'), ft | 0.79 | 1.25 |
| Effective passage length (L), ft | 0.71 | 1.17 |
| Fluid passage gap (d), ft | 0.0175 | 0.0233 |
| Number of passages (n) | 17 | 16 |
| No-flow dimension (L _N), ft | 0.762 | 0.762 |
| Minimum free area (A _c), sq ft | 0.321 | 0.264 |
| Equivalent diameter (D _e), ft | 0.0325 | 0.045 |
| Heat-transfer area (S), sq ft | 28.6 | 28.6 |
| Weight rate per unit free area in core (G _c = W/A _c), lb/(hr)(sq ft) | 12900 | 12100 |
| Reynolds number (Re = G _c D _e /μ) | 8550 | 5450 |
| Nusselt number (Nu = hD _e /k = 0.02 Re ^{0.8}) | 28 | 19.5 |
| Surface heat-transfer coefficient (h = Nu k/D _e), Btu/(hr)(sq ft)(°F) | 14.6 | 19.5 |
| ³ Over-all heat-transfer coefficient ($U = \frac{1}{\frac{1}{h_a} + \frac{1}{h_g}}$), Btu/(hr)(sq ft)(°F) | | 8.35 |
| Heat output (Q = USΔt _L), Btu/hr | | 305,000 |
| TOTAL-PRESSURE DROP OF CORE AT 18,000 FEET | | |
| Friction factor (f from reference 11) | 0.009 | 0.01 |
| Average velocity head in core [q _{av} = (G _c /3600) ² × 1/2gγ _{av}], lb/sq ft | 6.12 | 16.9 |
| 4L/D _e | 87.5 | 104 |
| Friction pressure drop (Δp _F = f q _{av} 4L/D _e), lb/sq ft | 4.82 | 17.5 |
| Outlet area (A ₅), sq ft | 0.99 | 0.50 |
| Expansion factor K _E = (1 - A ₄ /A ₅) ² | 0.457 | 0.224 |
| Velocity head at t ₄ [q ₄ = (G _c /3600) ² × 1/2gγ ₄], lb/sq ft | 7.61 | 15.50 |
| ⁴ Expansion-pressure drop (Δp _E = K _E q ₄), lb/sq ft | 3.48 | 3.47 |
| Velocity head at t ₃ [q ₃ = (G _c /3600) ² × 1/2gγ ₃], lb/sq ft | 4.61 | 18.1 |
| ⁵ Momentum-pressure drop (q ₄ - q ₃), lb/sq ft | 3.00 | -2.60 |
| Total-pressure drop of core Δp _C = Δp _F + Δp _E + (q ₄ - q ₃), lb/sq ft | 11.30 | 18.37 |

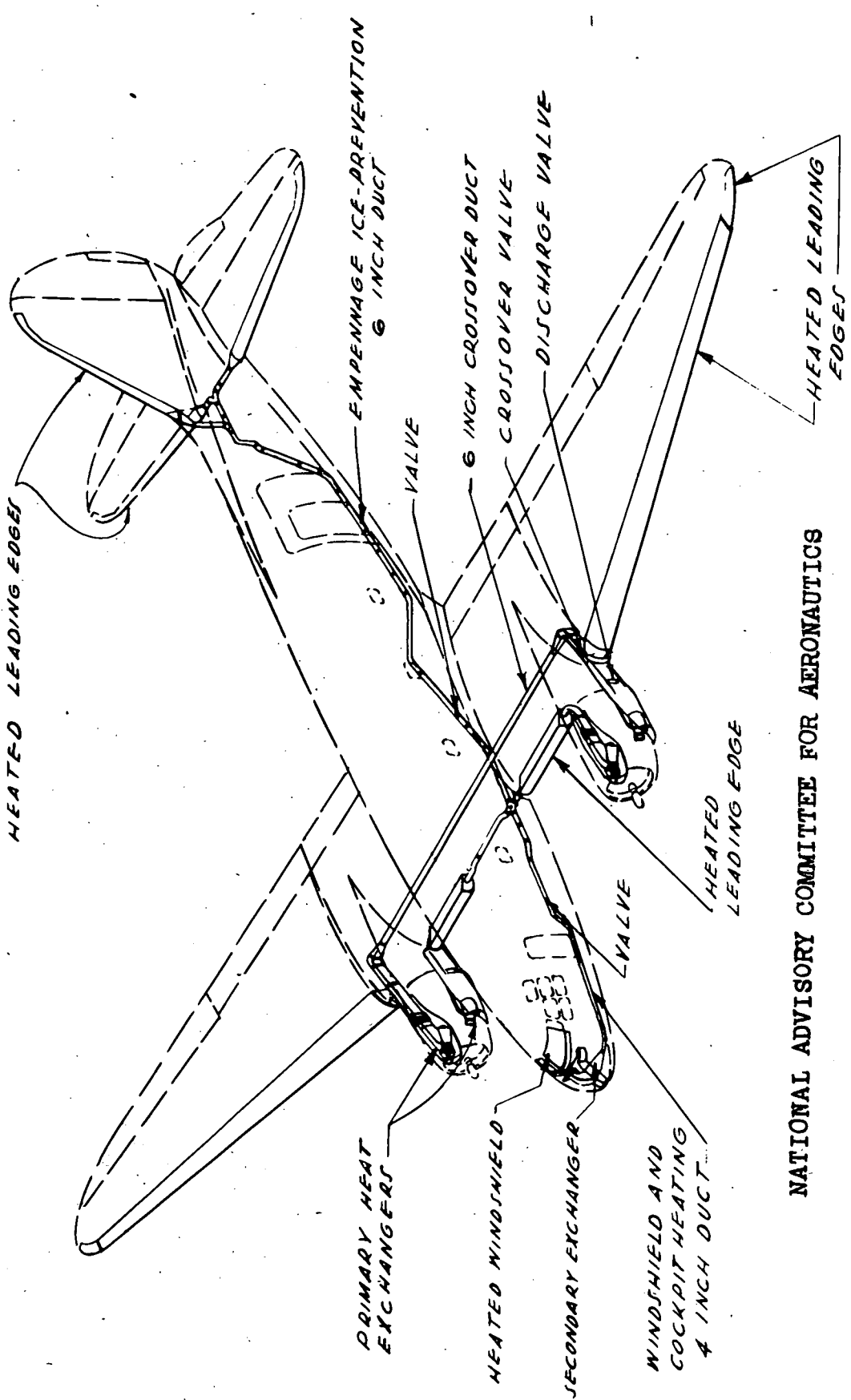
¹The numerical subscripts refer to the air-side stations shown in fig. 13 and to equivalent gas-side stations.

²It is assumed that the cross-flow correction factor is equivalent to unity.

³The thermal resistance of the metal walls is negligible.

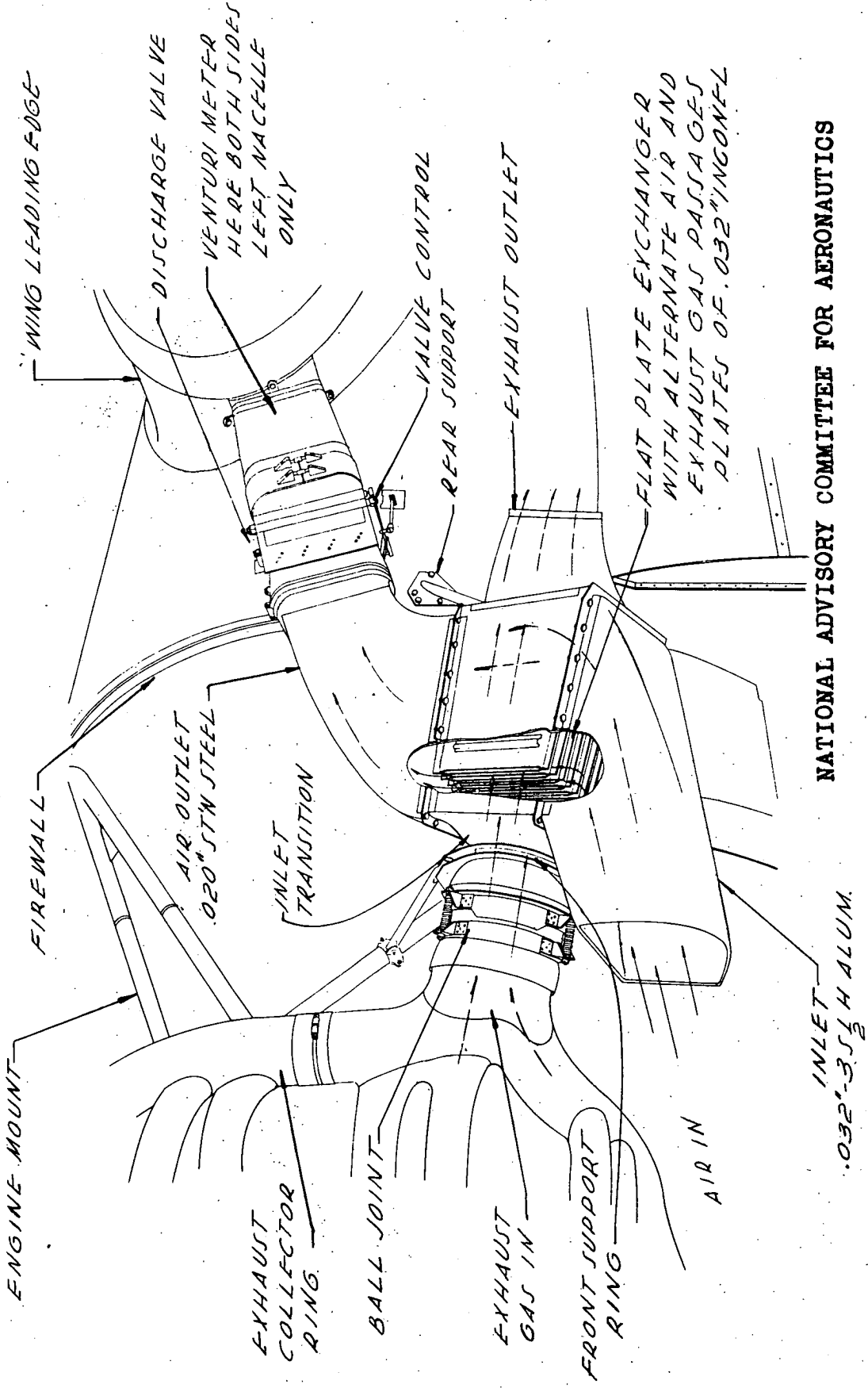
⁴The expansion loss in a 90° diverging channel is approximately the same as that in an abrupt expansion.

⁵This apparent drop in air-side total pressure is not necessarily a loss of energy. It may be recovered in the form of total pressure, provided the air is cooled to its original temperature at the same Reynolds number. Although it is probable that it is partially recovered in the system aft of the heat exchanger, it is slightly conservative to consider (q₄ - q₃) as a real loss in available ram.



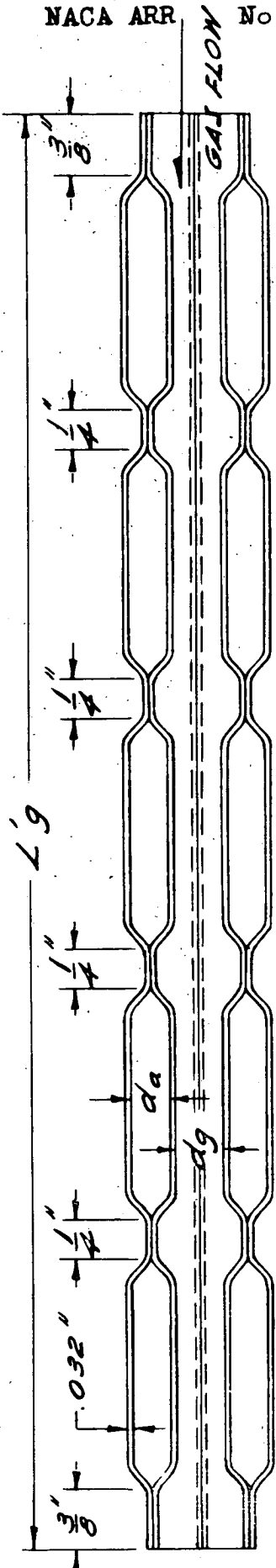
NATIONAL ADVISORY COMMITTEE FOR AERONAUTICS

FIGURE 1 - GENERAL ARRANGEMENT OF THE THERMAL ICE-PREVENTION SYSTEM FOR THE C-46 AIRPLANE



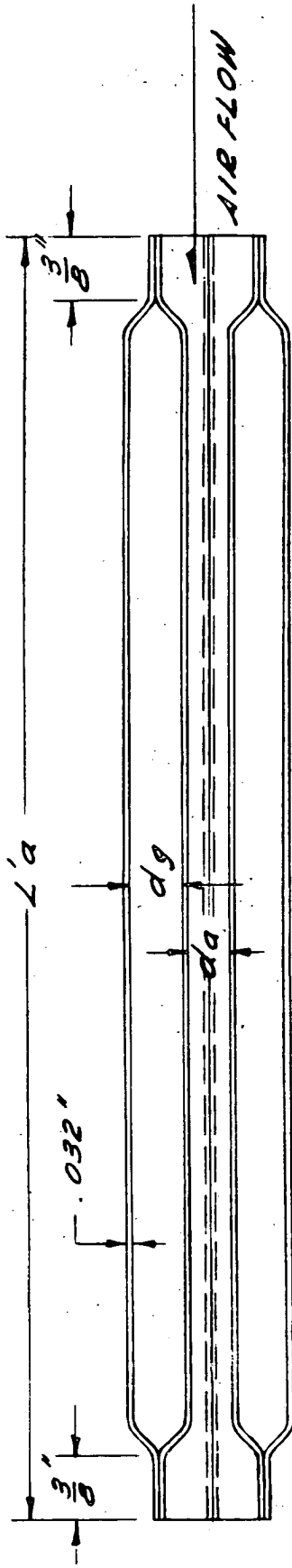
NATIONAL ADVISORY COMMITTEE FOR AERONAUTICS

FIGURE 2.- LOCATION OF THE HEAT EXCHANGERS ON THE C-46 AIRPLANE.



TYPICAL AIR PASSAGES

NATIONAL ADVISORY COMMITTEE FOR AERONAUTICS



TYPICAL GAS PASSAGES

FIGURE 3. - TYPICAL AIR AND GAS PASSAGES USED IN THE DESIGN OF THE HEAT EXCHANGER FOR THE C-46 AIRPLANE

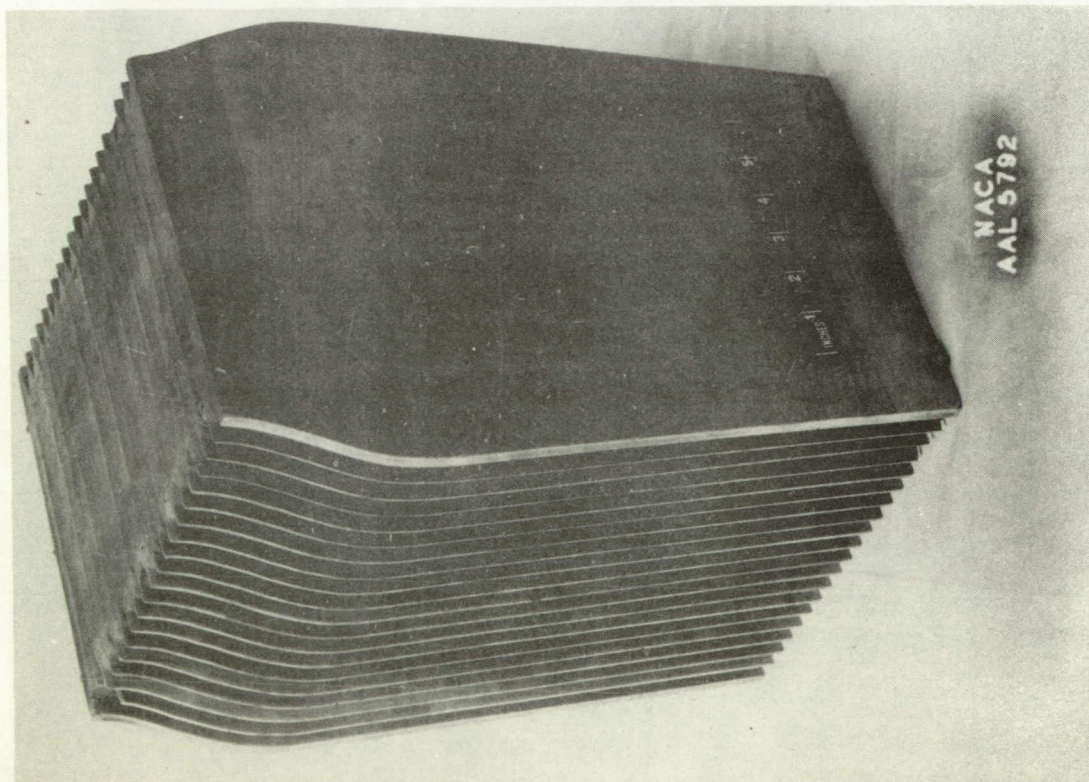
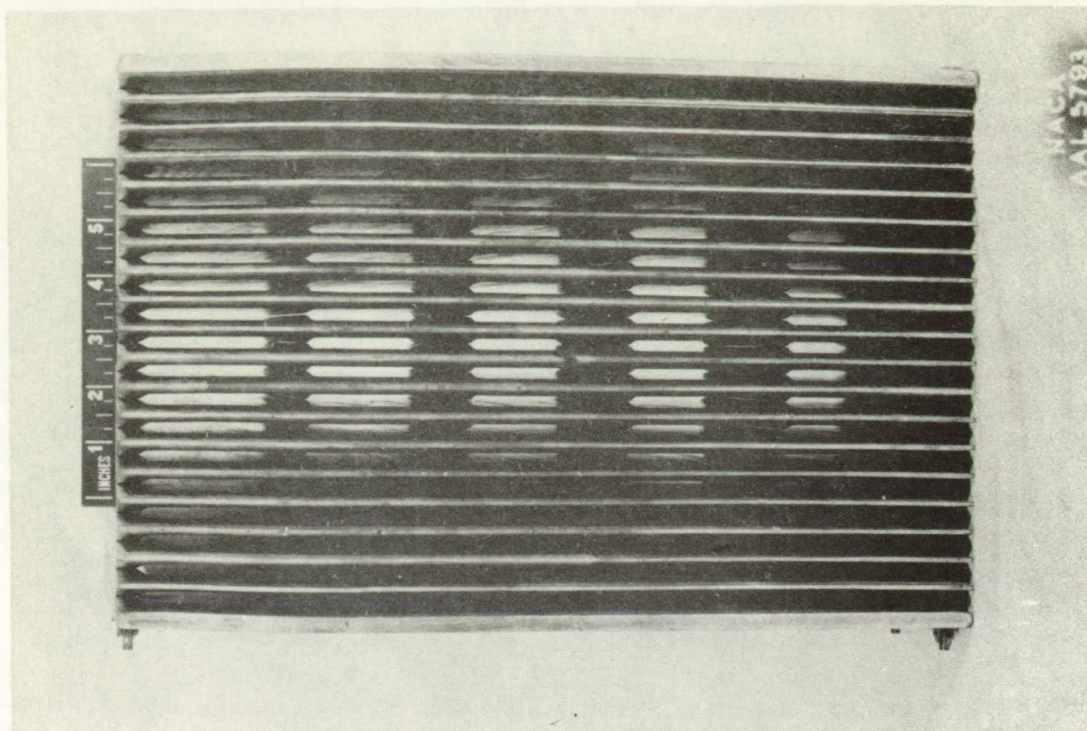


Figure 4.- Wood mock-up of heat exchanger, model 1, for the C-46 airplane.

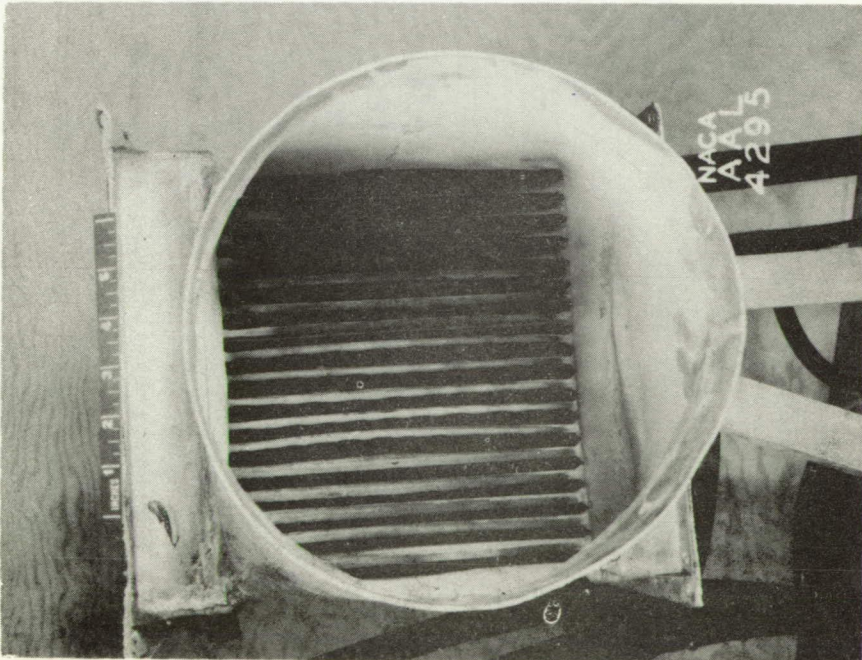
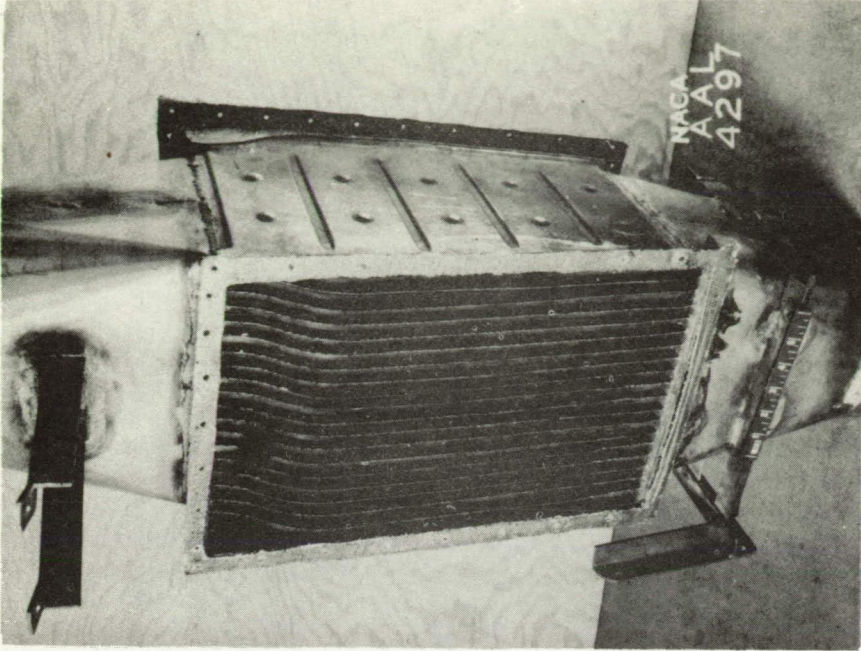


Figure 5.- Heat exchanger, model 1, for the C-46 airplane.

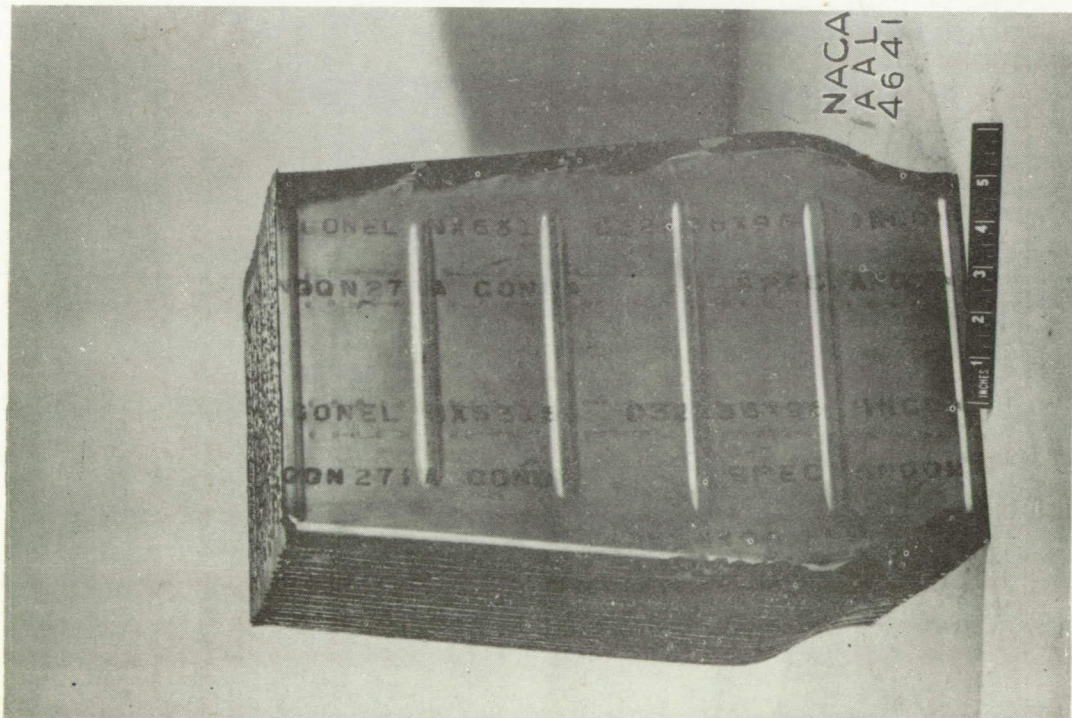
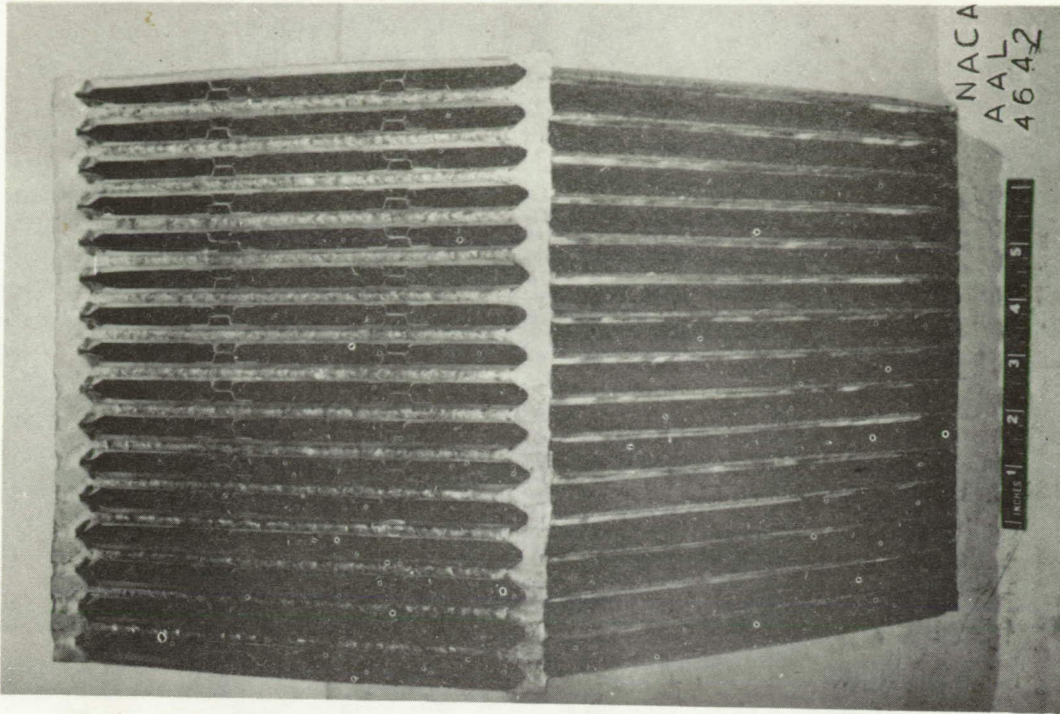


Figure 7.- Heat-exchanger core, model 2, for the C-46 airplane.

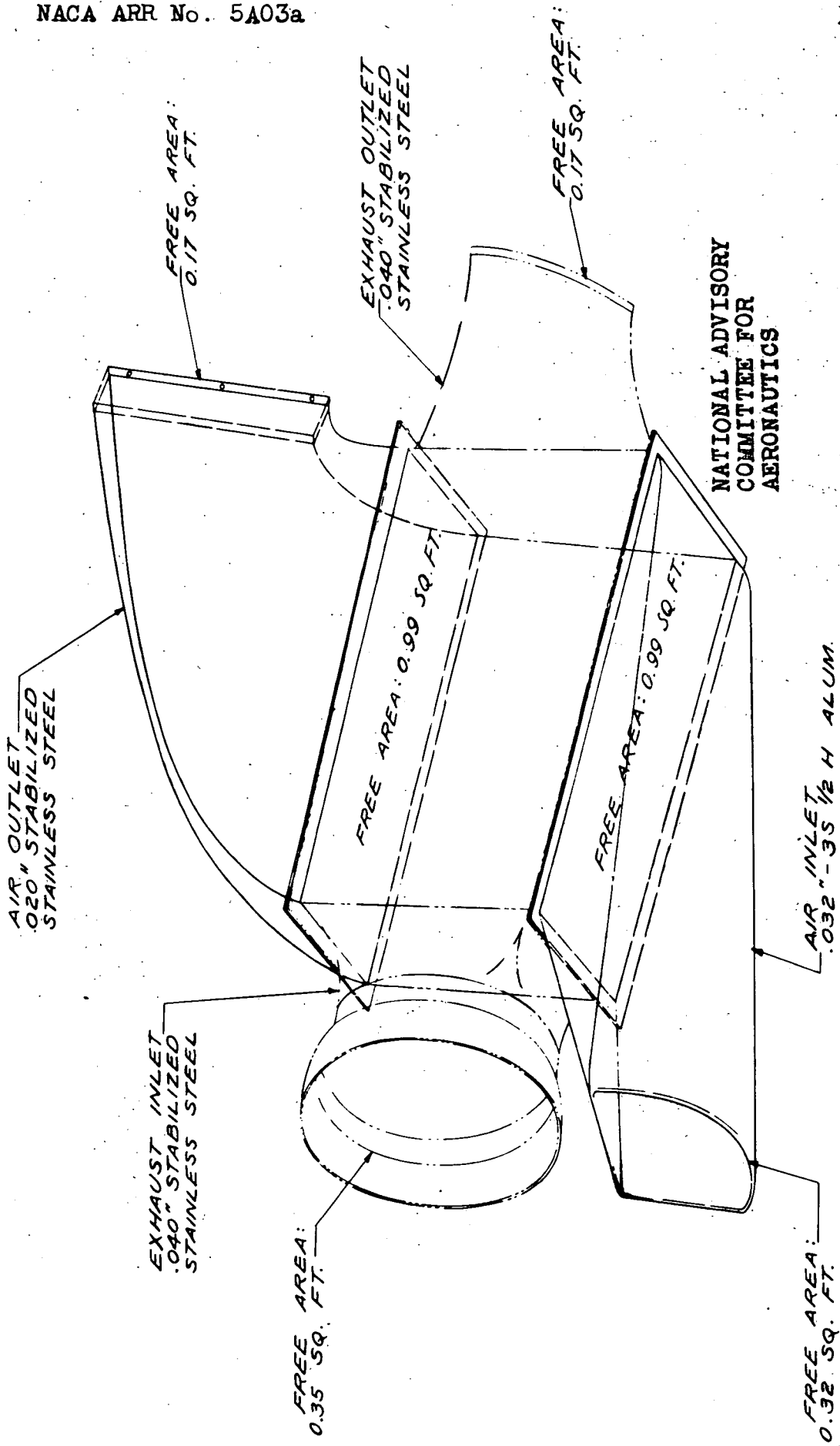


FIGURE 8. - INLET AND OUTLET HEADERS USED
IN THE HEAT-EXCHANGER INSTALLATION
ON THE C-46 AIRPLANE

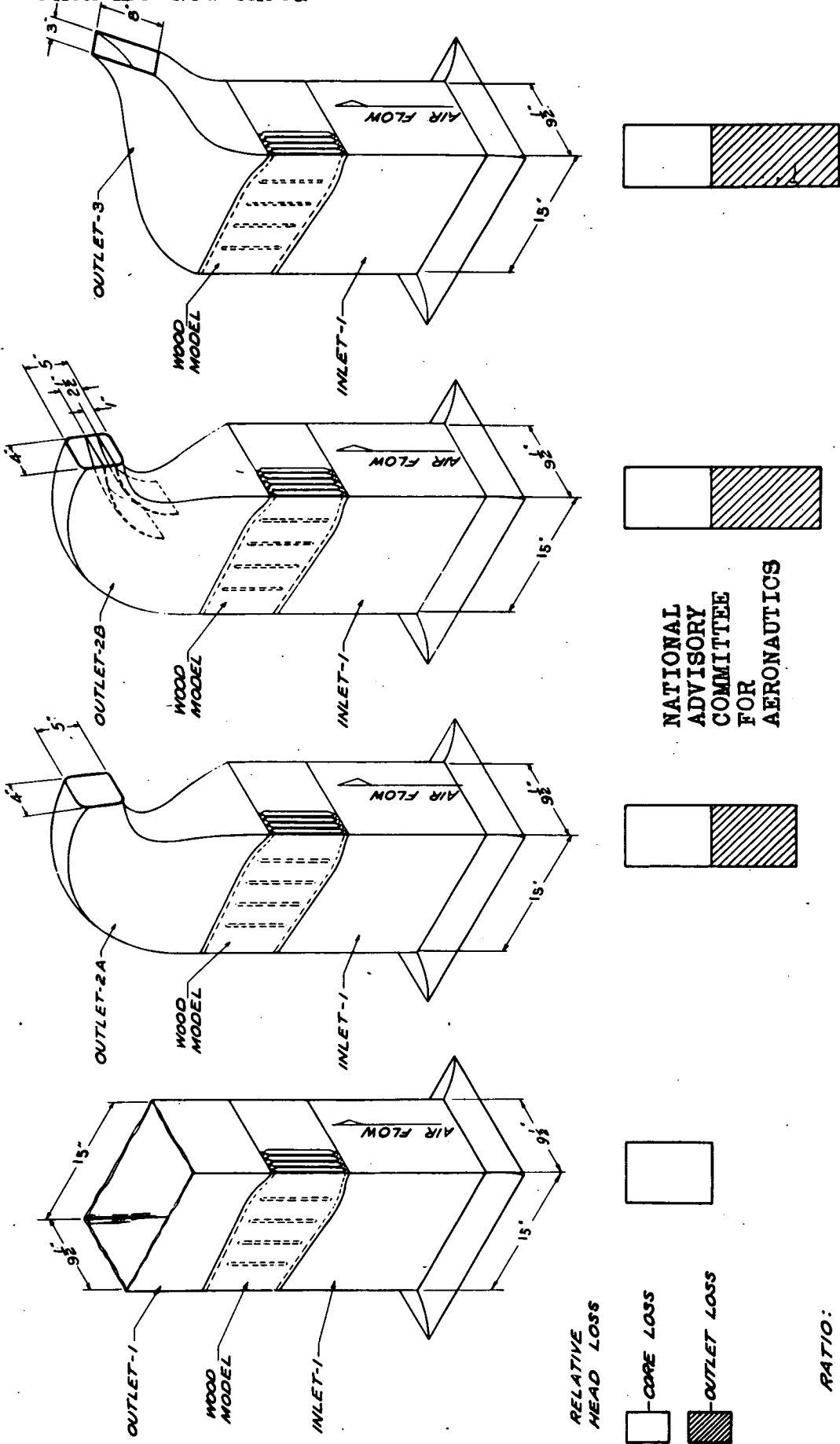
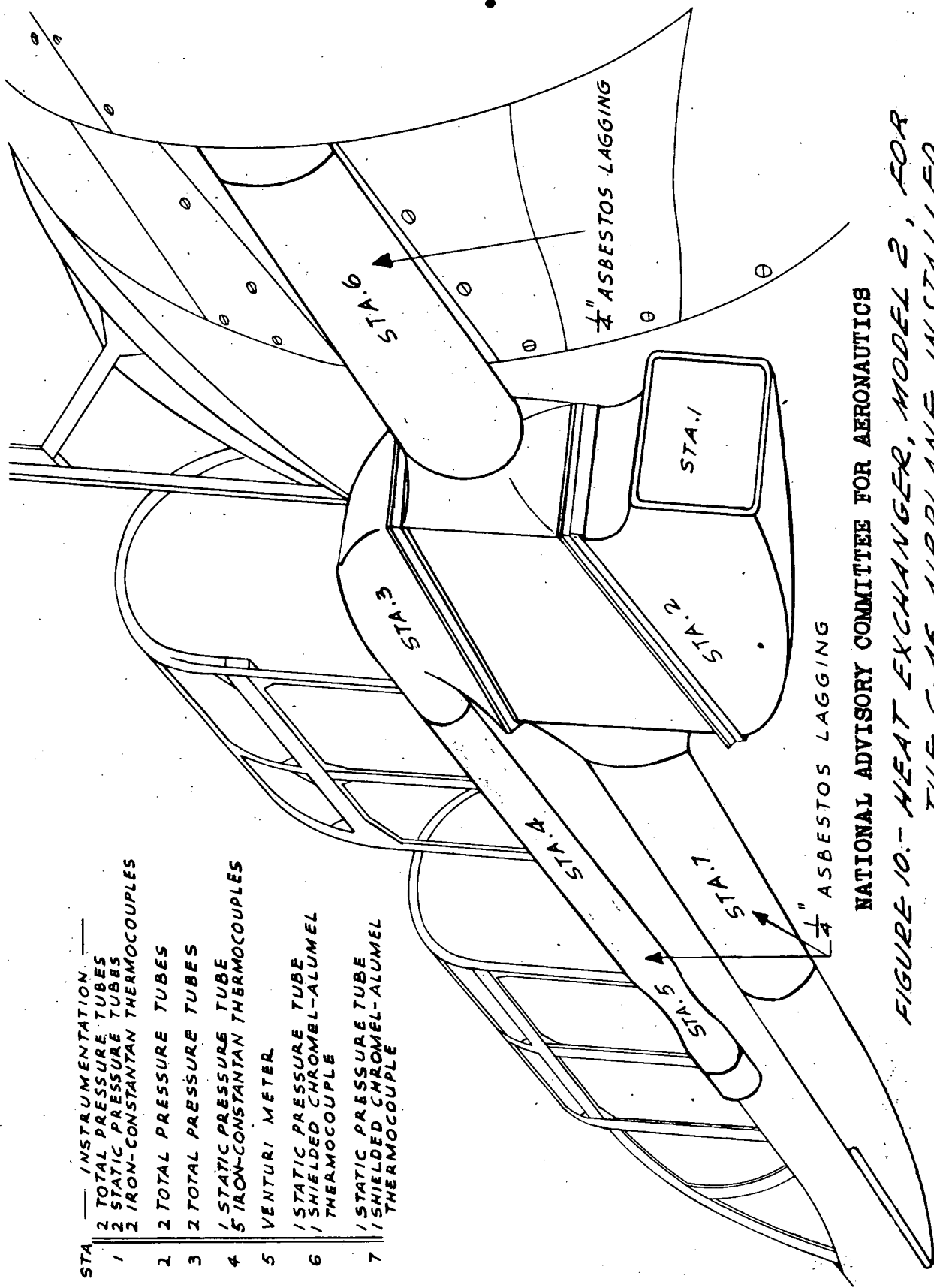


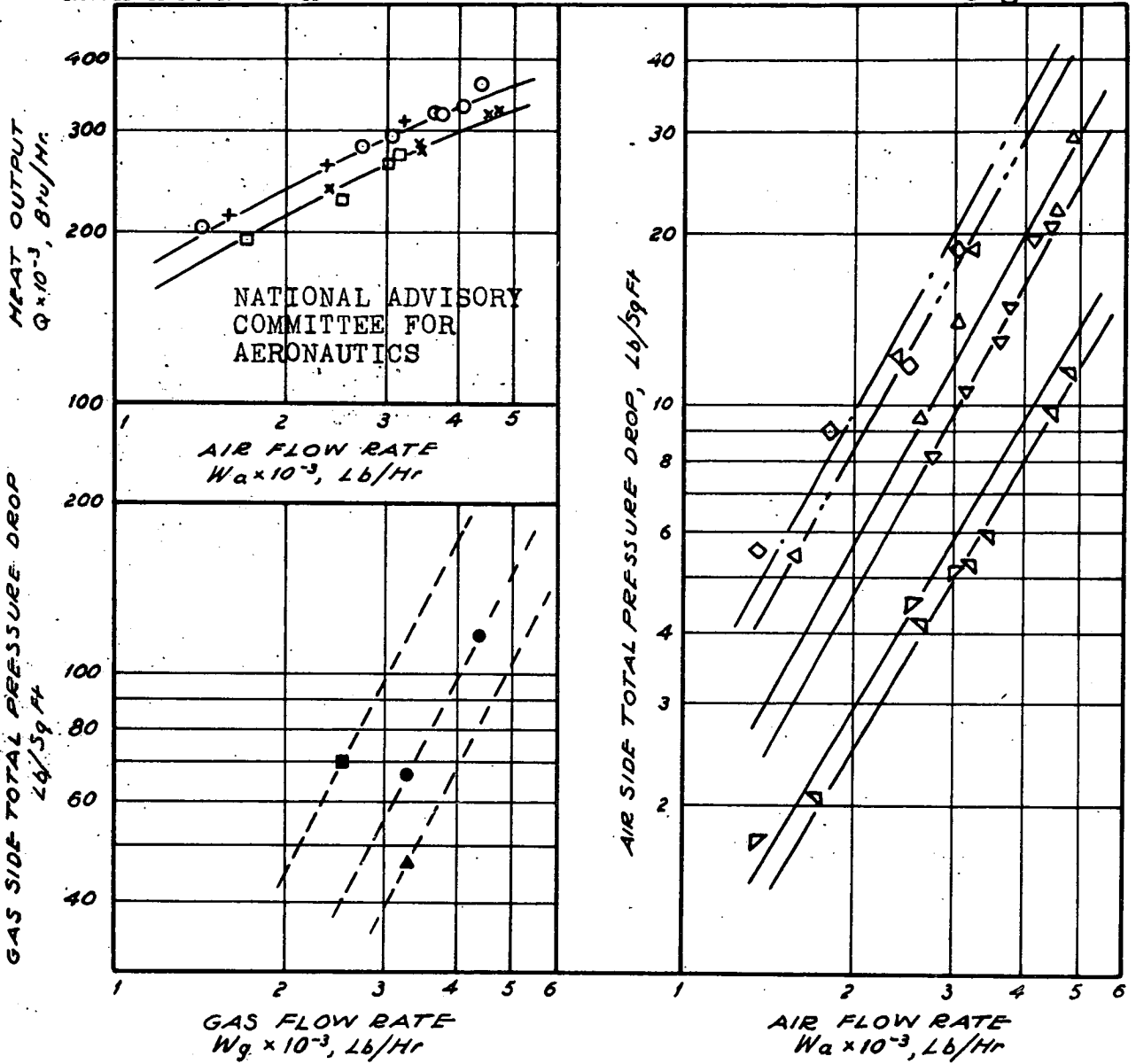
FIGURE 9. - A COMPARISON OF THE RELATIVE MERIT OF THREE OUTLET HEADERS USED IN THE SELECTION OF THE FINAL HEADER FOR INSTALLATION ON THE C-46 AIRPLANE.



- | | |
|------|--|
| STA. | INSTRUMENTATION. |
| 1 | 2 TOTAL PRESSURE TUBES |
| 2 | 2 STATIC PRESSURE TUBES |
| 3 | 2 IRON-CONSTANTAN THERMOCOUPLES |
| 4 | 2 TOTAL PRESSURE TUBES |
| 5 | 2 TOTAL PRESSURE TUBES |
| 6 | 1 STATIC PRESSURE TUBE |
| 7 | 5 IRON-CONSTANTAN THERMOCOUPLES |
| | VENTURI METER |
| | 1 STATIC PRESSURE TUBE |
| | 1 SHIELDED CHROMEL-ALUMEL THERMOCOUPLE |
| | 1 STATIC PRESSURE TUBE |
| | 1 SHIELDED CHROMEL-ALUMEL THERMOCOUPLE |

NATIONAL ADVISORY COMMITTEE FOR AERONAUTICS

FIGURE 10.- HEAT EXCHANGER, MODEL 2, FOR THE C-46 AIRPLANE, INSTALLED FOR TESTS ON AN O-47A AIRPLANE



HEAT OUTPUT

- — MODEL I AT 5000 FEET
- + — MODEL I AT 18000 FEET
- x — MODEL II AT 5000 FEET
- — MODEL II AT 18000 FEET

TEST CONDITIONS

- $W_g = 3300$ Lb/Hr, $t_{g_{in}} = 1600^\circ\text{F}$, $t_{a_{in}} = 50-60^\circ\text{F}$
- $W_g = 3300$ Lb/Hr, $t_{g_{in}} = 1600^\circ\text{F}$, $t_{a_{in}} = 18^\circ\text{F}$
- $W_g = 3300$ Lb/Hr, $t_{g_{in}} = 1600^\circ\text{F}$, $t_{a_{in}} = 60-70^\circ\text{F}$
- $W_g = 2500$ Lb/Hr, $t_{g_{in}} = 1600^\circ\text{F}$, $t_{a_{in}} = 30^\circ\text{F}$

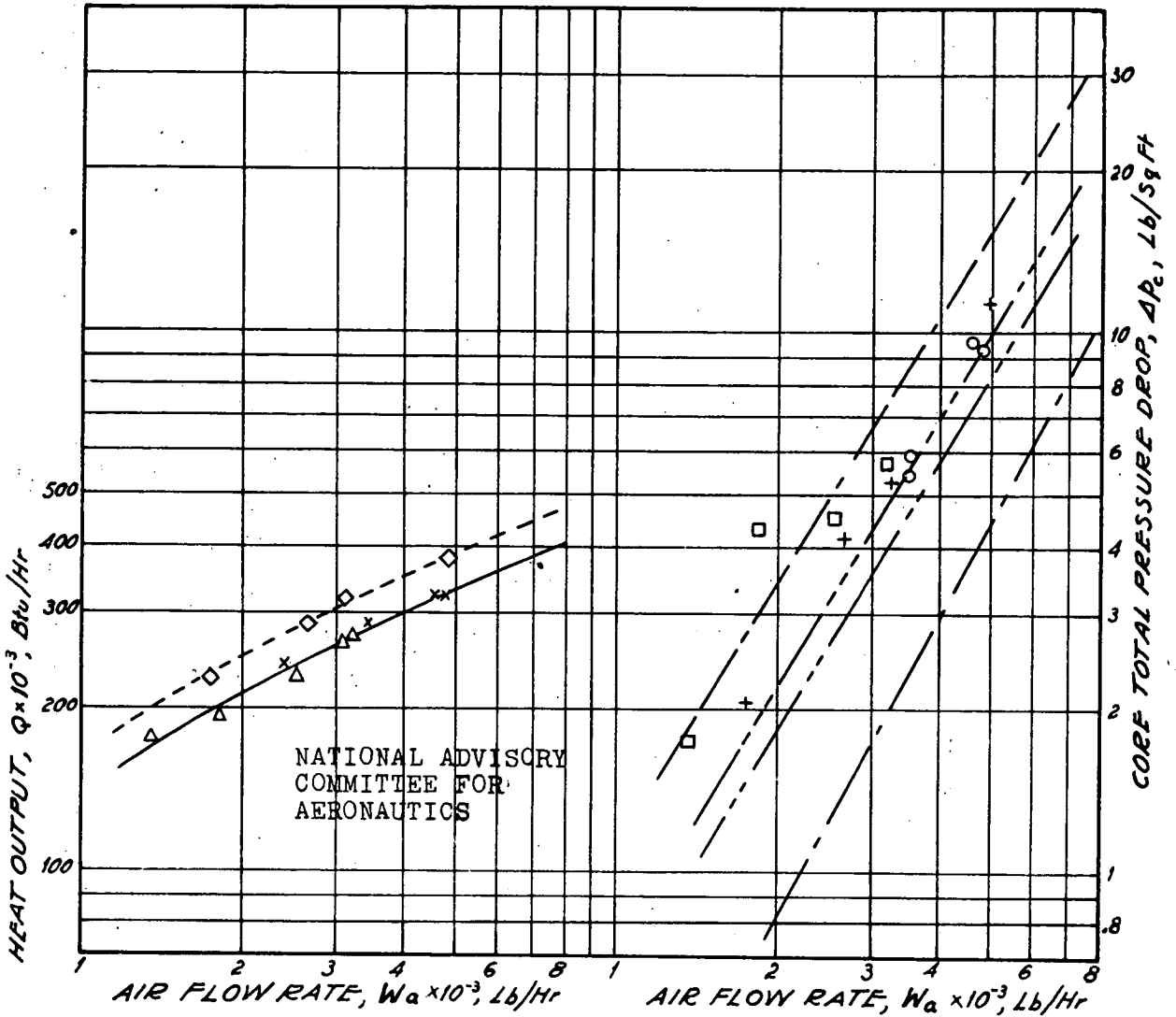
AIR SIDE TOTAL PRESSURE DROP, Δp_a

- ◇--- MODEL II, OVERALL Δp_a AT 18000 FEET
- △--- MODEL II, OVERALL Δp_a AT 5000 FEET
- ▽--- MODEL II, CORE Δp_a AT 18000 FEET
- △--- MODEL II, CORE Δp_a AT 5000 FEET
- ◇--- MODEL I, OVERALL Δp_a AT 18000 FEET
- ▽--- MODEL I, OVERALL Δp_a AT 5000 FEET

GAS SIDE TOTAL PRESSURE DROP, Δp_g

- MODEL II, OVERALL Δp_g AT 18000 FEET
- MODEL II, OVERALL Δp_g AT 5000 FEET
- ▲--- MODEL I, OVERALL Δp_g AT 5000 FEET

FIGURE 11.— MEASURED PERFORMANCE OF HEAT EXCHANGER, MODELS 1 AND 2, DESIGNED FOR THE C-46 AIRPLANE AND TESTED ON AN O-47A AIRPLANE



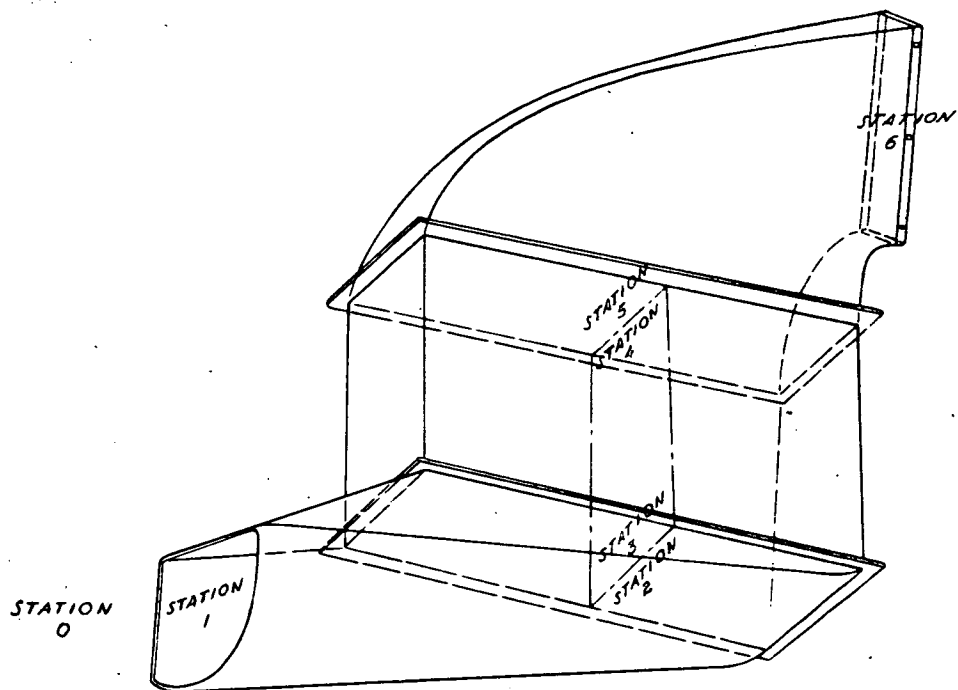
HEAT OUTPUT

- CALCULATED, DESIGN CONDITIONS
- x MEASURED AT 5000 FEET, $W_g = 3300$ Lb/Hr
- Δ MEASURED AT 18000 FEET, $W_g = 2500$ Lb/Hr
- ◇— MEASURED AT 5000 FEET, $W_g = 4400$ Lb/Hr

CORE TOTAL PRESSURE DROP

- — — CALCULATED, ISOTHERMAL AT SEA LEVEL, STD. COND.
- — — CALCULATED, NON-ISOTHERMAL AT SEA LEVEL, STD. COND.
- · — · — CALCULATED, NON-ISOTHERMAL AT 5000 FEET, STD. COND.
- o MEASURED, NON-ISOTHERMAL AT 5000 FEET, $W_g = 3300$ Lb/Hr
- + MEASURED, NON-ISOTHERMAL AT 5000 FEET, $W_g = 4400$ Lb/Hr
- MEASURED, NON-ISOTHERMAL AT 18000 FEET, $W_g = 2500$ Lb/Hr
- · — · — CALCULATED, NON-ISOTHERMAL AT 18000 FEET, STD. COND.

FIGURE 12.— A COMPARISON BETWEEN CALCULATED AND MEASURED HEAT OUTPUT AND AIR-SIDE PRESSURE DROP OF THE HEAT-EXCHANGER CORE, MODEL 2, USED ON THE C-46 AIRPLANE



NATIONAL ADVISORY COMMITTEE FOR AERONAUTICS

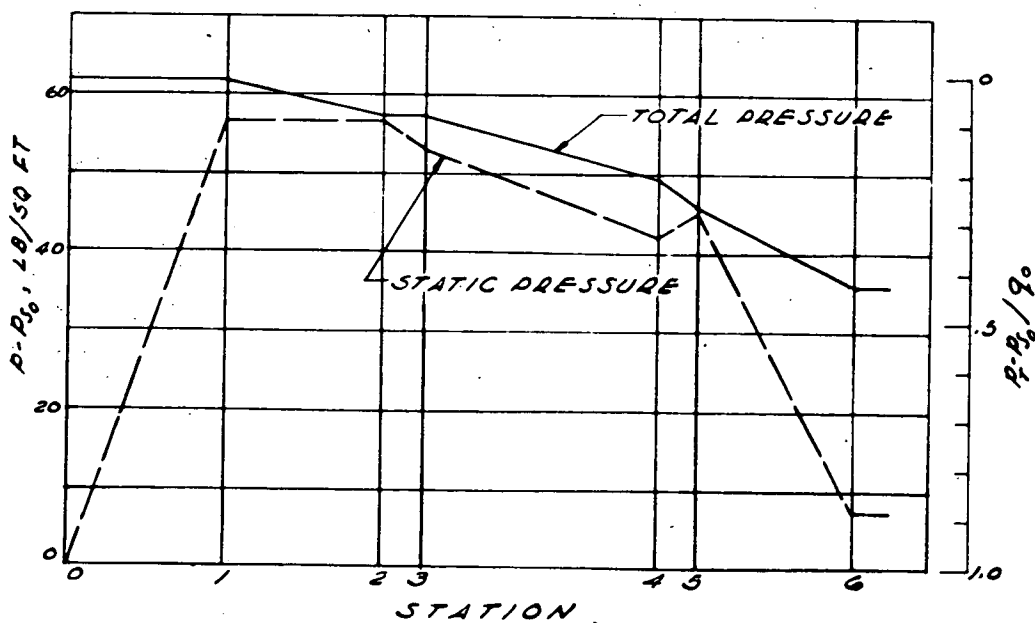


FIGURE 13.- DISTRIBUTION OF PRESSURE LOSSES IN THE HEAT-EXCHANGER INSTALLATION ON THE C-46 AIRPLANE WHILE CRUISING AT 18,000 FEET